THE MAINTENANCE OF SHARPNESS IN MAGNIFIED DIGITAL IMAGES

by

James David Fahnestock

A Thesis Submitted to the Faculty of the

DEPARTMENT OF SYSTEMS AND INDUSTRIAL ENGINEERING

In Partial Fulfillment of the Requirements
For the Degree of

MASTER OF SCIENCE
WITH A MAJOR IN SYSTEMS ENGINEERING

In the Graduate College

THE UNIVERSITY OF ARIZONA

1 9 8 1

STATEMENT BY AUTHOR

This thesis has been submitted in partial fulfillment of requirements for an advanced degree at The University of Arizona and is deposited in the University Library to be made available to borrowers under rules of the Library.

Brief quotations from this thesis are allowable without special permission, provided that accurate acknowledgment of source is made. Requests for permission for extended quotation from or reproduction of this manuscript in whole or in part may be granted by the head of the major department or the Dean of the Graduate College when in his judgment the proposed use of the material is in the interests of scholarship. In all other instances, however, permission must be obtained from the author.

SIGNED: James D. Palmstock

APPROVAL BY THESIS DIRECTOR

This thesis has been approved on the date shown below:

B. R. Hunt

B. R. HUNT
Professor of
Electrical Engineering

12-16-81
Date

ACKNOWLEDGMENTS

This thesis is the culmination of a year of graduate study in systems engineering with emphasis on digital image processing.

The completion of this work was spurred by the enthusiastic interest expressed in the subject by my advisor, Dr. Bobby R. Hunt. Much of the background needed to formalize the techniques described herein would not have been found if it were not for his broad knowledge of the digital image processing literature.

Much of my working knowledge of image processing used in this paper is attributed to my association with Dr. Robert Schowengerdt, who aided me considerably during Dr. Hunt's absence.

Finally, I would like to recognize my mother, Betty Fahnestock, for her diligent efforts during the completion of this paper. Her proofreading of this manuscript was undaunting, even in the face of a few paragraphs for which she did not have the foggiest understanding.

TABLE OF CONTENTS

LIST OF ILLUSTRATIONS

LIST OF TABLES

ABSTRACT

The large amounts of digital image data now becoming available make softcopy imagery exploitation a desirable capability. One aspect of digital imagery exploitation, image magnification is studied. Two filtering techniques to maintain image sharpness as digital images are enlarged are developed. The most promising technique includes the use of a model of the retina of the eye. An example is presented which illustrates the definition of frequency domain filters to satisfy the objective of sharpness maintenance.

CHAPTER 1

INTRODUCTION

With the recent advances in electronics and solid-state detectors the collection of image data in digital form is becoming commonplace. With this onslaught of digital image data it is anticipated that the need for equipment to efficiently exploit the wealth of information in this imagery will be seen.

Image exploitation by photographic interpreters or analysts is a flourishing business, and the tools used in the process have evolved over many years. It is assumed that the current image exploitation equipment gives a good basis for the capabilities that will be desired in softcopy, cathode ray tube (CRT), equipment for the exploitation of digital image data. Such functions as image magnification or zoom, image rotation, image sharpness or focus, and image scanning will be needed. Each of these functions is relatively easily and aptly accomplished by currently available exploitation equipment but can be considerably more difficult to implement in hardware or software for softcopy exploitation.

This study addresses only one of these functions, image magnification. The subtle problems encountered when

an attempt is made to simulate the analog function of zoom of a microscope in a digital system will be considered. An attempt will be made to insure constant sharpness of the perceived image as the magnification is changed. The system components will be described in the frequency domain. This description will aid the development of a technique to provide a constant image power spectrum regardless of magnification.

Since the objective is the maintenance of visual sharpness it is necessary to consider the human visual system in developing a viable technique. Several models of the spatial characteristics of vision have been constructed (Mannos and Sakrison 1974; Hall and Hall 1977; Granrath 1979). The usefulness of these models is entrenched in their explanation of the performance of human vision in engineering terms. In this way these models can aid the solution to engineering problems that involve human vision. Many problems only require a model whose output is a reasonable portrayal of vision while others benefit from a model which more closely resembles the physiological structure and functioning of the eye.

The Granrath Model (Granrath 1979) embodies this second quality and therefore seems most applicable in this effort. It includes nonlinearities which seem to represent the eye well and divides the viewed image into a high pass and low pass image. This last characteristic of the

Granrath Model is of particular interest since it is primarily the high frequencies that control image sharpness. The high pass output from this model is used to develop the proper filter function to maintain image sharpness as the image is magnified (Figure 1.1).

A basic method for objectively determining the visual quality of an image has been discussed by Hunt and Sera (1978). The area under the product of the eye modulation transfer function (MTF) and the modulus of the Fourier transform of the perceived brightness image has been shown to relate well to perceived image quality. Since image sharpness can change the perceived quality of an image it is believed that a relationship exists between image sharpness and the modulus of the image Fourier transform. In fact, the use of high gain filters to make images appear sharper is based on this concept.

Typically, the modulus of the Fourier transform of an image is a monotonically decreasing function with increasing frequency. As the image is magnified the size of the image details increase on the retina of the eye. Effectively, this represents a shift to lower frequences of those modulus amplitudes initially found at higher frequencies (Figure 1.2). This then represents a degradation of the perceived image as evidenced by the reduced area under the eye MTF and image transform modulus product curve (Hunt and Sera 1978).

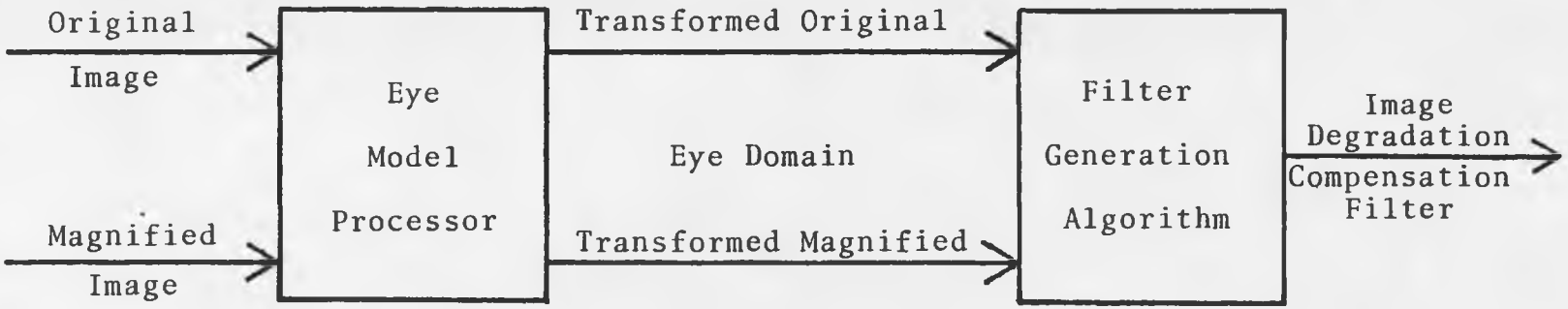

Figure 1.1 An Eye Model Used to Aid
Image Restoration Filter Definition

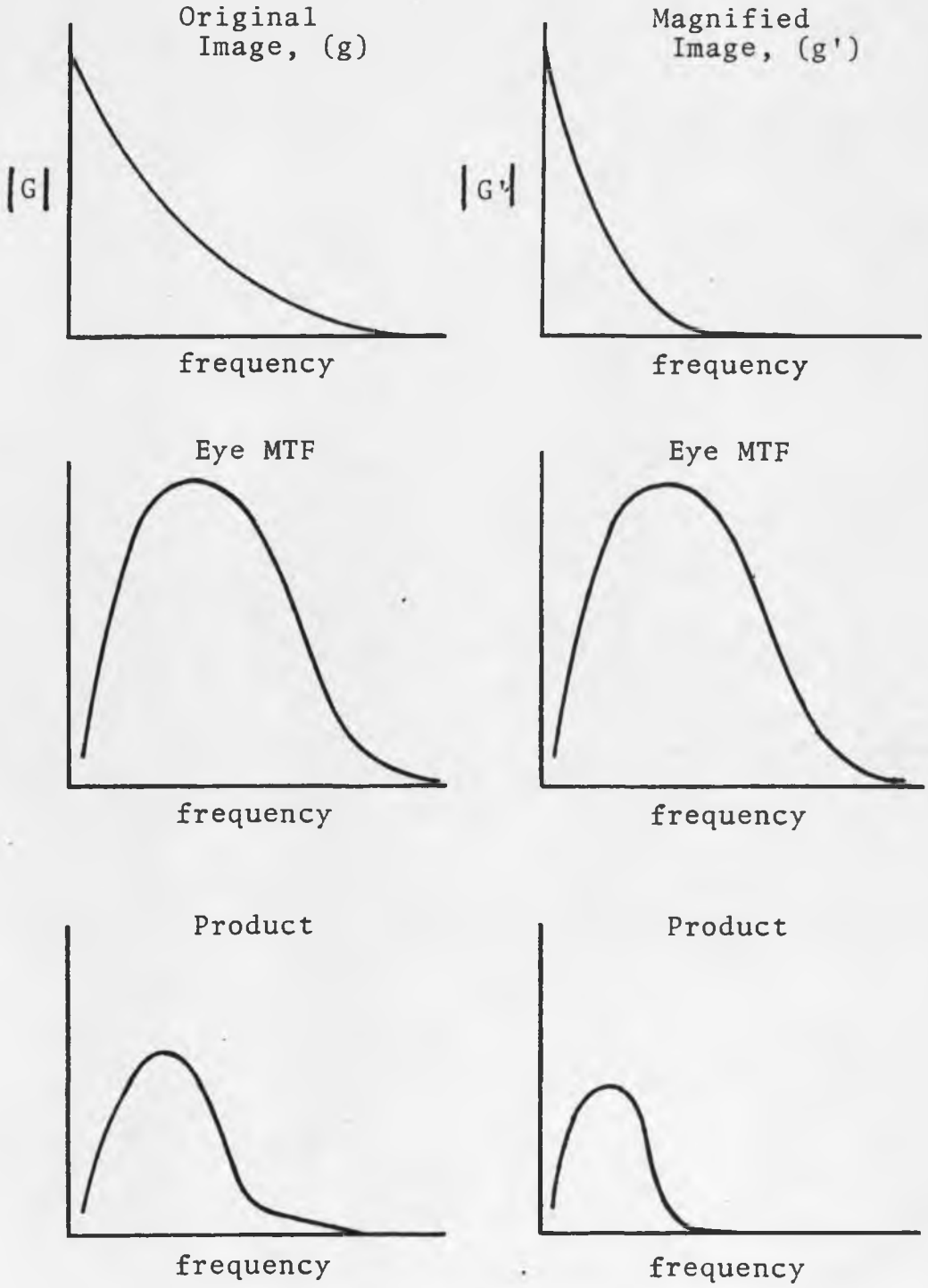

Figure 1.2 Perceived Degradation due to Image Magnification

An intuitive approach would be to apply a filter to the magnified image that would increase it's transform modulus to that of the original image. This would require a filter whose value, in the frequency domain, is greater than one at all frequencies other then zero (Figure 1.3). When applied, this type of filter causes not only a sharpening of the image but considerable changes to the observed tonal characteristics.

A second approach is to design a filter which affects only the higher frequencies of the image. This then will be less likely to cause noticeable tonal changes which are related to lower image frequencies, yet provide the desired image sharpening. The question then becomes how to decide on the filter characteristics and over what frequency range should it operate? The Granrath Model will be used to circumvent this problem. The high pass image output from the model will define the frequency range being operated upon. The difference between the model high pass outputs for the original image and the magnified image will be used to define the functional form of the filter.

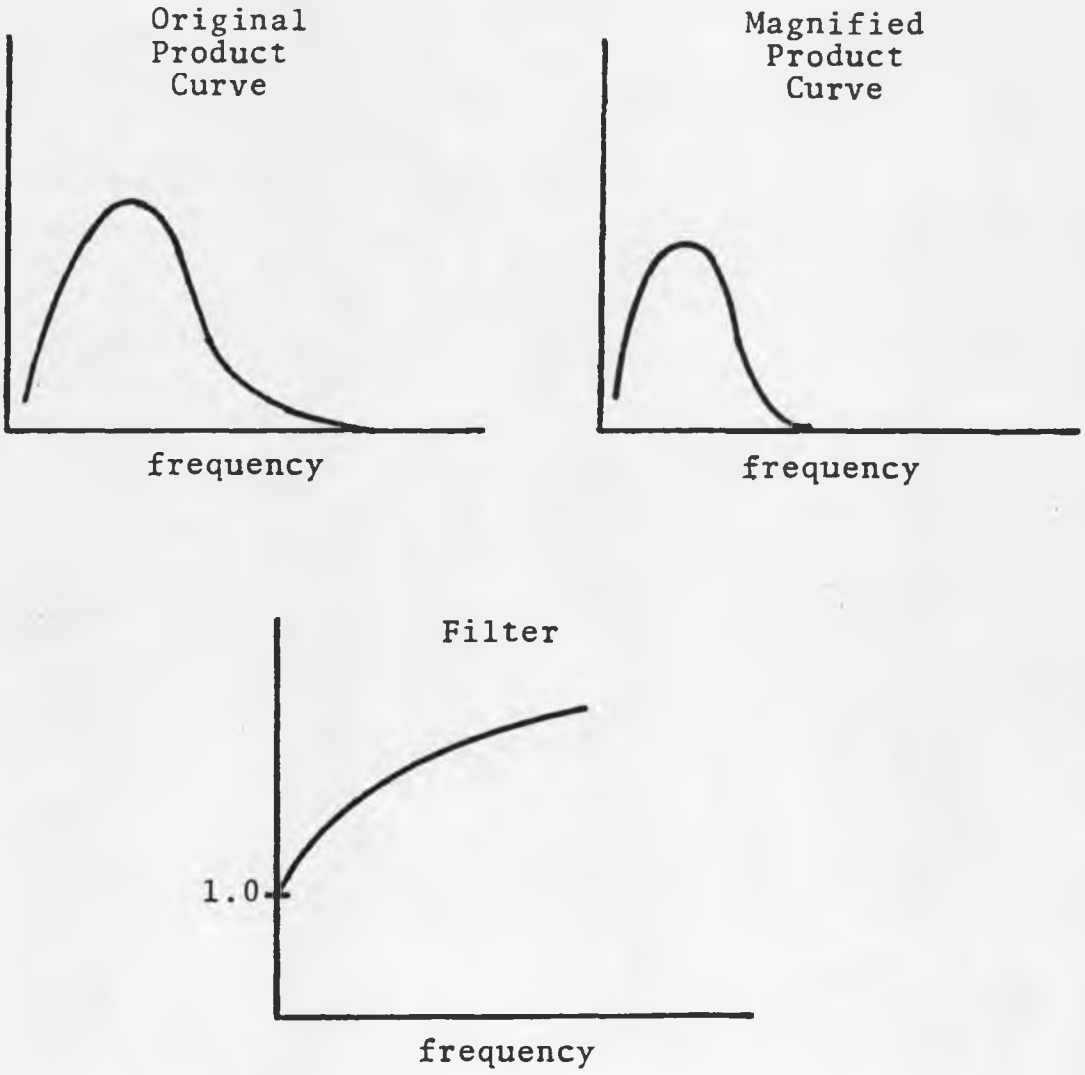

Figure 1.3 Intuitive Filter Design

CHAPTER 2

GRANRATH TWO-CHANNEL MODEL OF THE RETINA

There is evidence that the retina of the eye breaks an image down into two components, one low spatial frequency and one higher spatial frequency. Additionally, it appears that both of these components are transmitted via the optic nerve to higher vision centers in the brain (Legge 1978). The Granrath Two-Channel Model of the retina takes advantage of this concept in deriving its functional form.

The model is portrayed in Figure 2.1. It is generally accepted that perceived brightness is a nonlinear function of the image intensity. In this model the natural logarithm is used as the nonlinearity:

$$x_{ij} = \log(1+u_{ij}) \quad , \qquad (2\text{-}1)$$

where u_{ij} is the input image and x_{ij} is the brightness image in the receptor cells. It has been argued that the Steven's Power Law with a 0.33 exponent should be used to model the retina's intensity to perceived brightness transformation. Both the logarithm and power law functions perform compression of the data with similar results. The major difference is in the prediction of perceived contrast. If Steven's Power Law is used it is predicted that small equal intensity

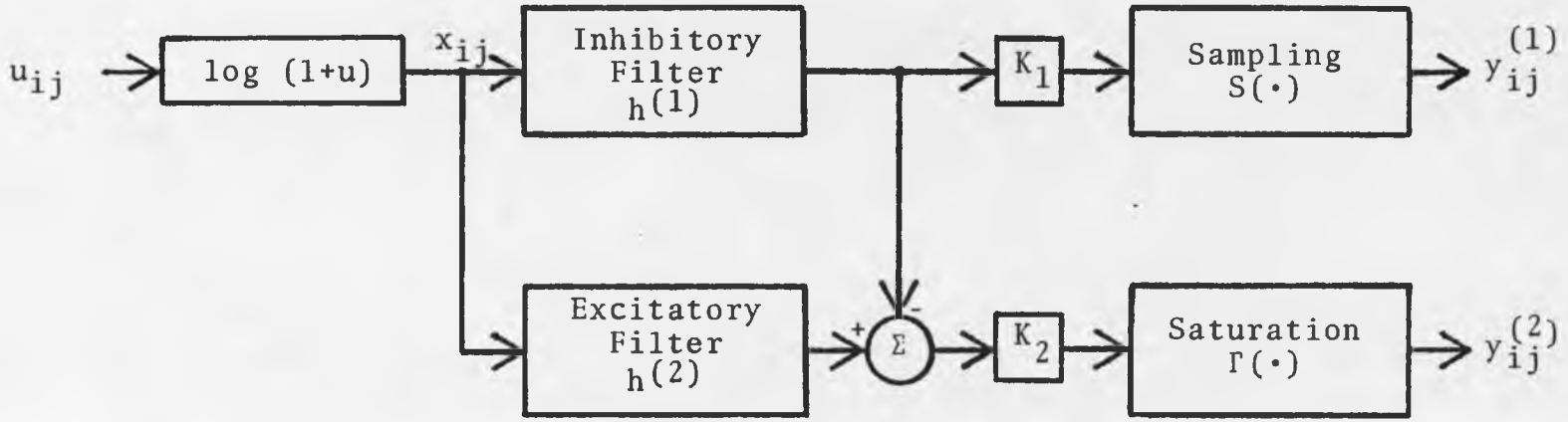

Figure 2.1 A Two-Channel Model of Spatial Interaction in the Human Retina (from Granrath 1979)

contrasts at different intensity levels will be equally perceived, while a log law predicts that small contrasts will be modified by a factor of $\ln^{-1}$ of the intensity level.

Once the image is transformed into the perceived brightness domain it is broken down into two components by the inhibitory filter and the excitatory filter. The inhibitory filter is a low pass filter which represents the spacial averaging that appears to be accomplished by certain cells in the retina. This low pass image is sampled and transmitted to higher vision centers in the brain and also used within the retina of the eye to perform further image processing. The sampling operator $S(\circ)$ is used to model the sampling of the low pass retina output. The excitatory filter is a low pass filter but has a higher cutoff frequency then the inhibitory filter. Its output represents the direct output from the receptors in the retina. The difference between the output from the two filters is formed by cells within the retina. The magnitude of this difference image is limited by the saturation levels of the cells. This limiting or clipping is modeled by the saturation operator $\Gamma(\circ)$. The output is then transmitted to the brain.

The two channels of the model can be represented by the following two equations:

$$y_{ij}^{(1)} = S\{K_1 \Sigma\Sigma h_{k,\ell}^{(1)} \circ x_{i-k,j-\ell}\} \qquad (2\text{-}2)$$

$$y_{ij}^{(2)} = \Gamma\{K_2(\Sigma\Sigma h_{mn}^{(2)} \circ x_{i-m,j-n} - \Sigma\Sigma h_{k\ell}^{(1)} \circ x_{i-k,j-\ell})\} \quad . \quad (2\text{-}3)$$

K_1 and K_2 are constants which model different channel gains and $h_{k,\ell}$ and $h_{m,n}$ are Gaussian type weighting functions.

$$h_{k,\ell}^{(1,2)} = \frac{C_{1,2} \exp\{-(k^2+\ell^2)/p_{1,2}^2\}}{\Sigma\Sigma_{k\ell} \exp\{-(k^2+\ell^2)/p_{1,2}^2\}} \quad (2\text{-}4)$$

These two dimensional weighting functions are radially symmetric. This is an approximation since the retina is somewhat anisotropic.

Granrath (1979) found values for the constants of K_1=1.0, p_1=5.0, C_1=1.0, K_2=3.0, p_2=0.5, C_2=1.0; the filter size K=15 which gives $-7 \leq k \leq 7$ and $-7 \leq \ell \leq 7$ for both filters; and saturation at ±1.0 ($S(\circ)=\pm 1.0$) to provide results which represent the functioning of the retina near the fovea. Granrath and Hunt (1979) suggested that the saturation levels $S(\circ)$ be set at ±1/6 the maximum image brightness range.

Figure 2.2 shows the weighting functions $h^{(1)}$ and $h^{(2)}$ that result from use of the values listed above. Since both weighting functions have the same dimensions they can be combined to form a single weighting function for calculating $y^{(2)}$. This combined weighting function is shown in Figure 2.3. An example of the calculations related to implementing this model can be found in Appendix A.

INHIBITORY (CHANNEL 1)

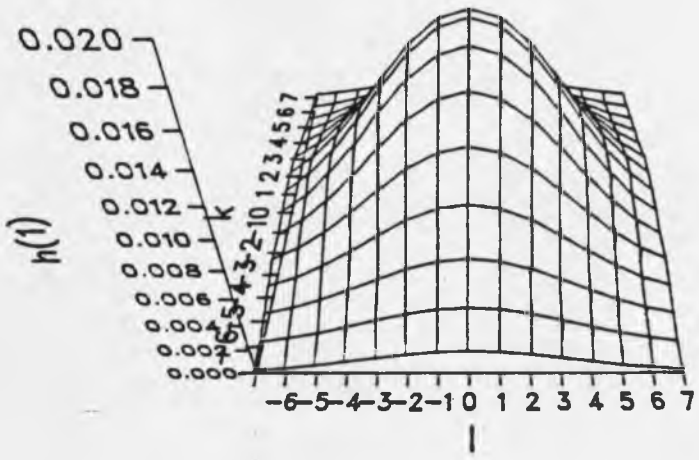

EXCITATORY

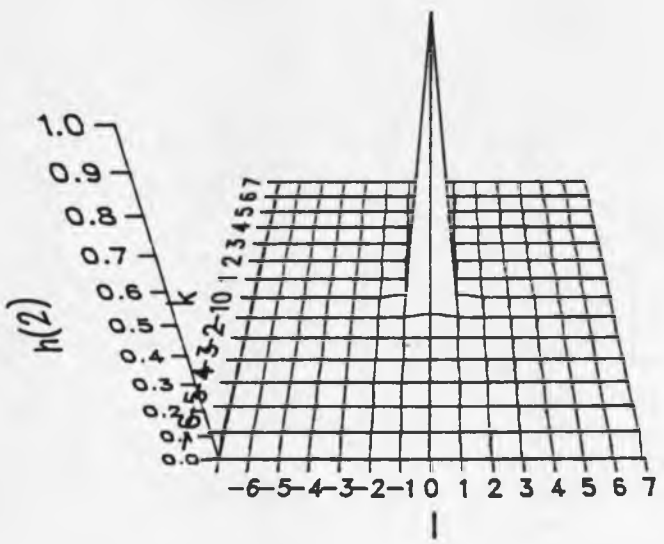

Figure 2.2 Weighting Functions

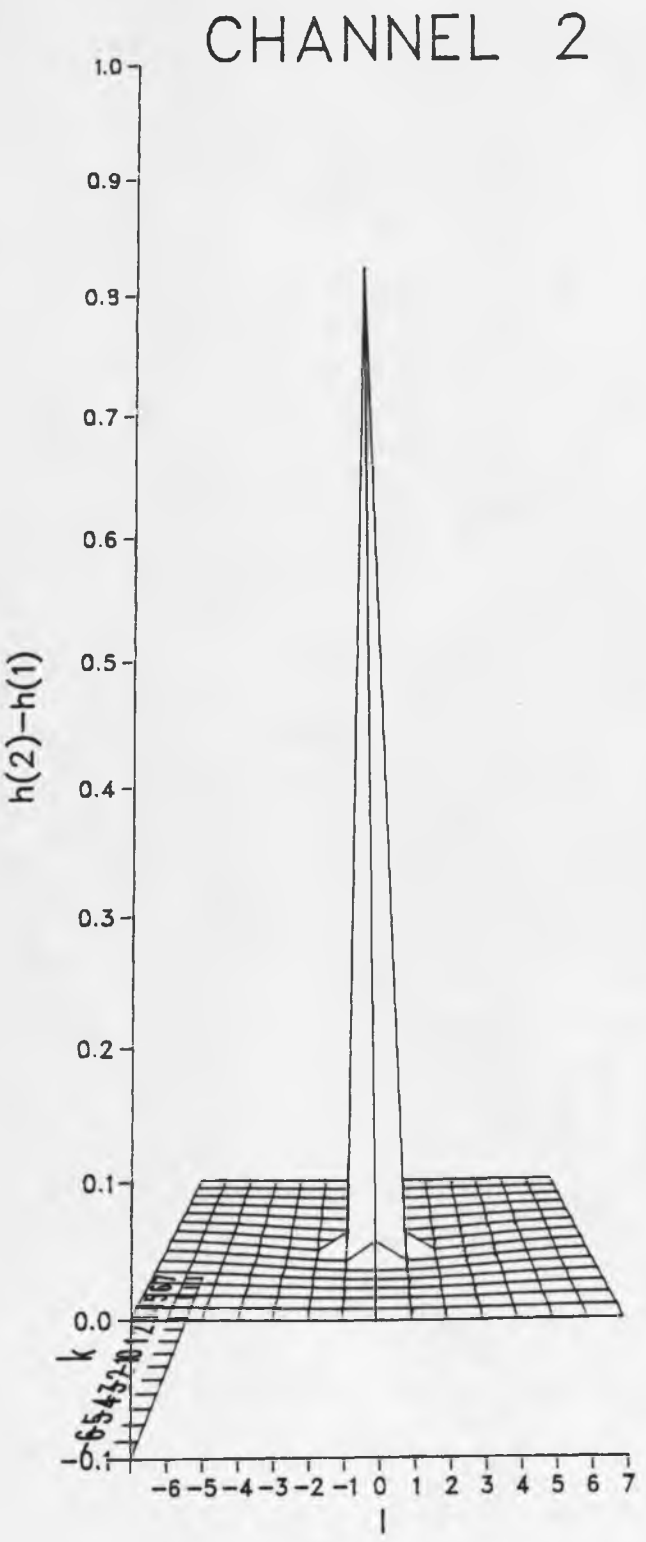

Figure 2.3 Combined Weighting Function

CHAPTER 3

IMAGE MAGNIFICATION AND DEGRADATION COMPENSATION

There are several techniques used to magnify digital images. They are all based on the estimation of pixel intensity values for pixels at positions between the original sampled points. This chapter identifies some of the techniques and provides the reasoning for selecting bilinear interpolation for use in this paper.

The basic concepts related to the restoration of magnified images are presented in chapter 1. A simple approach to this restoration is investigated here. A more complex restoration procedure based on the Granrath Model discussed in chapter 2 is developed to overcome some of the shortfalls of the simple approach.

3.1 Magnification Techniques

Digital image magnification is typically accomplished by using one of several techniques. The nearest neighbor approach is very simple, but its simplicity limits its usefulness. The approach is to determine the coordinates of the output pixels relative to the input pixels. The intensity value for an output pixel is then the value of the closest input pixel. The assumption here is that the input image is uniform in the area surrounding a pixel. It is obvious that for images where the intensity variation from pixel to pixel is significant this technique is not adequate.

Another common approach is bilinear interpolation. This technique does not assume a uniform input image in the neighborhood of a pixel. Instead, it assumes that the intensity value for any location within an image can be determined from the intensity values of the four pixels surrounding the point of interest. A weighted average of the four relevent input pixel intensity values is used to represent the new output pixel intensity value. This, in essence, is the use of an interpolation function which is triangular in one dimension or pyramidal in two dimensions.

If the original input image was band-limited and the sampling of that image was carried out properly then the

original image could be reconstructed exactly, using the sinc function $\left(\frac{\sin\pi X}{\pi X}\right)$ as the interpolation function. Since the sampling function must be truncated in order to provide a finite image for image processing the original image can not be perfectly reconstructed. The error is usually negligible at distances of more than eight to ten Nyquist samples from the edge (Pratt 1978). However, the infinite extent of the sinc function makes exact use of it impossible.

Other interpolation functions, such as the bell, cubic B-spline and Gaussian, have been discussed in the literature. These functions are more complex to implement than bilinear interpolation but do provide some advantages. They are less difficult to work with than the sinc function. However, due to the complexity of the image restoration algorithm developed in this work it was desired to use a relatively simple interpolation technique to reduce the overall complexity in the processing required to magnify an image. For this reason bilinear interpolation is used throughout. Any degradation of the image due to use of this technique will be considered part of the degradation of enlargement and will be compensated for by the restoration technique.

3.2 Bilinear Interpolation

Let us first examine linear interpolation in one dimension. Consider a set of data consisting of pairs of numbers, each pair describing a data point. The first number of the pair represents a location along an axis in one dimension. The second number represents the amplitude of a function at that point. In order to estimate the value of the function between any two of the data points, linear interpolation can be used.

In Figure 3.1a the value of the function at point C is being estimated. First, the relative distance from A to C is determined by

$$\text{relative distance} = \frac{C-A}{B-A} \quad .$$

Next, the change in the value of the function from A to C can be determined.

$$\text{change in function} = (b-a)(\text{relative distance})$$

The value of the function at point C is then its value at point A plus the change from A to C.

$$c = a + \text{change in function}$$

$$c = a + (b-a)\frac{C-A}{B-A}$$

$$c = a + \frac{b-a}{B-A}(C-A)$$

It can be seen that (b-a)/(B-A) is the slope of the line

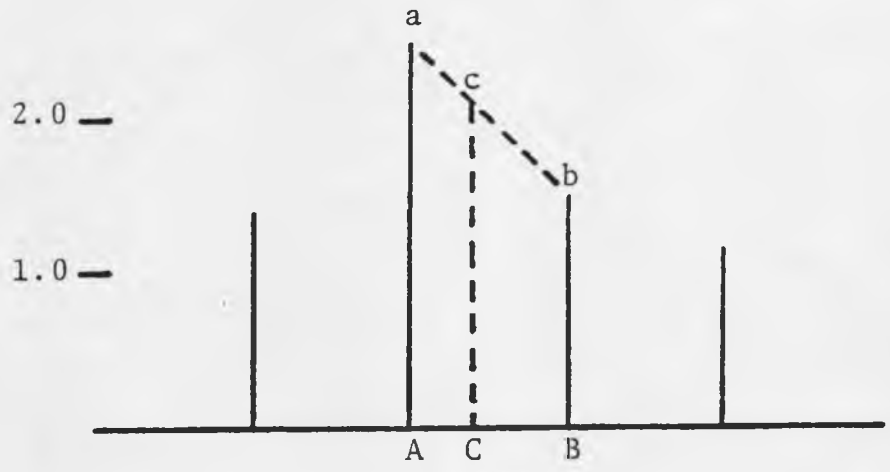

(a)

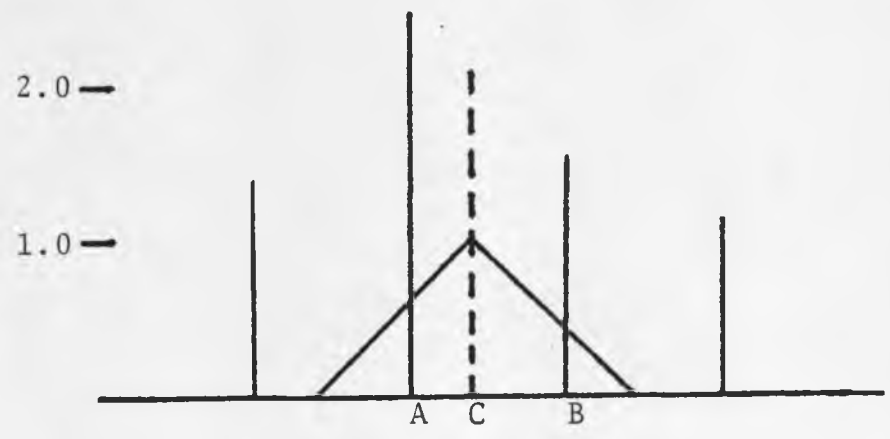

(b)

Figure 3.1 Linear Interpolation

between (A,a) and (B,b) and a provides the proper bias. Essentially, this is no more than the evaluation of a point on a line.

Another approach to interpolation is that of convolution (Figure 3.1b). A triangular convolution function can be used to provide the same results as above. The slopes of the sides of the convolution function are designed to provide a maximum height of 1.0 and total width of 2(B-A). The value of the function at the desired point can be found in the following way. First, place the peak of the convolution function at the desired point. Next, multiply the existing data points by the convolution function and sum the results. This sum is the estimated value of the function at the desired point and is identical to that obtained by linear interpolation. In this way the value at any point along the axis can be estimated.

Bilinear interpolation is similar to linear interpolation except that the existing data points lie in a two dimensional grid rather than on a one dimensional axis. One approach to the estimation of the value of the function at a point other than one of the input data points follows. If the estimated value of the function at point E in Figure 3.2a is desired, linear interpolation is used to estimate the function value at point F, using points A and B, and at point G, using points C and D (Figure 3.2b). Next, the function values at points F and G can be used in

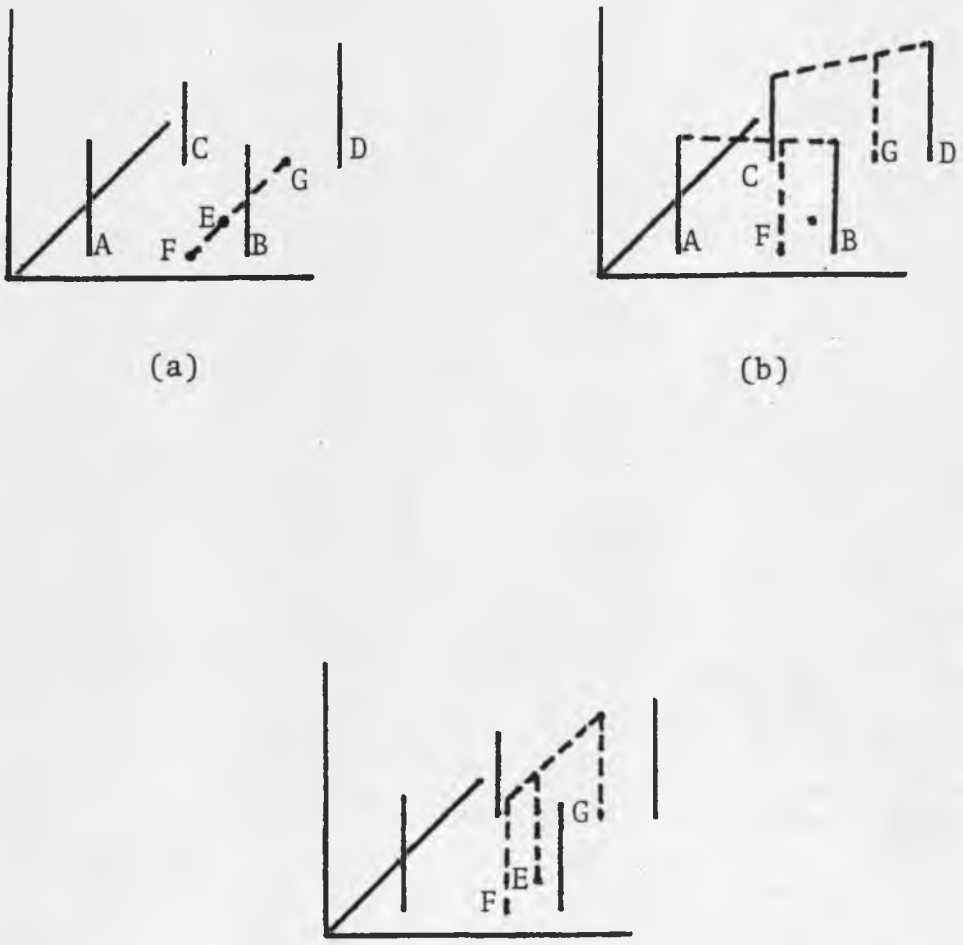

Figure 3.2 Bilinear Interpolation

a third linear interpolation to find the value at point E (Figure 3.2c).

A convolution approach similar to that used for linear interpolation can be used for bilinear interpolation. In this case, instead of using a triangular convolution function a pyramidal, two dimensional function is used.

3.3 Simple Filter Design Approach

This approach is based on homomorphic filtering as discussed by Andrews and Hunt (1977). The concept is to design a filter in the frequency domain based on an estimate of the power spectrum of the original object and the power spectrum of the recorded image. Since the power spectrum is the square of the modulus of the Fourier transform it is necessary first to take the square root of the spectra which gives the associated moduli. The quotient formed when the modulus of the original object is divided by the modulus of the recorded image is the magnitude of the desired filter. This technique specifies only the magnitude of the filter. In this study the phase will be assumed to be zero. If homomorphic filtering is correctly implemented the modulus of the Fourier transform of the resultant image should duplicate that of the original object.

A modification must be made in the filter design technique for use in this study. Instead of filtering a recorded image to produce an image whose power spectrum is equal to that of the original object, a magnified image is being filtered to provide an output image which has sharpness characteristics similar to those of the original image prior to magnification. Direct substitution of the original

image for the original object and the magnified image for the recorded image can not be made. In the magnification process objects get larger and their frequency content shifts towards lower frequencies. For this reason, when the moduli of the original and magnified images are divided a filter based on the differences in the same objects or object characteristics in the two images is no longer being designed. Therefore, it is not desirable to produce a filtered image whose power spectrum is exactly that of the original image. Instead, it is desired to produce a filtered magnified image that has a power spectrum that on the average is equal to that of the original image. This will provide a filtered image which insures equivalent stimulus to the eye as discussed by Hunt and Sera (1978).

The modulus of the Fourier transform of an image represents the relative frequency content of the image and also the orientation of the frequency components. Since images are two dimensional functions their transforms are also two dimensional. The distance a point in the Fourier transform lies from the origin or DC value of the transform is proportional to its associated frequency. Using this concept, a one dimensional radial average Fourier transform modulus can be formed by averaging modulus data points in annular rings centered at the origin. The width of the annular rings determines the amount of averaging performed

along the frequency axis. A width is selected that provides a smooth function so that only the general characteristics of the image power spectrum are maintained. Since annular windows define the domain over which averaging occurs, all angular information in the two dimensional transform modulus is removed and a one dimensional average modulus function is defined.

The average modulus functions for the original and magnified images are found. The resultant function from the original image is divided by the function from the magnified image. This defines the magnitude of the restoration filter in one dimension. To apply this filter to the two dimensional Fourier transform of the magnified image, rotational symmetry of the filter is assumed. This assumption is valid based on the fact that the filter was developed from data averaged in anular rings about the center of the transform.

There are some characteristics of this approach which cause unwanted results. These characteristics are discussed in chapter 4 and require the use of a more complex restoration procedure to affect the desired results.

3.4 Complex Filter Design Approach

This filter design technique is similar to that described in section 3.3. The added complexity comes from the preprocessing of the original and magnified images to provide images that represent the high frequency output of the eye. By doing this preprocessing the differences in the average modulus functions between the original and magnified images represent the differences in the perceived sharpness of the images. Designing the filter in this way insures that the sharpness of the magnified image, after filtering, is maintained without unwanted changes in the overall contrast.

The image preprocessing that is applied is that associated with channel 2 of the Granrath Model described in chapter 2. Due to the nature of the Granrath Model the filter resulting from this complex design technique must be applied to the logarithm of the magnified image. This precludes the expression of the filter in the spatial domain and its combination with the interpolation function. If this combination were possible then the magnification and filtering could be accomplished simultaneously.

CHAPTER 4

APPLIED FILTER DESIGN

The digital image processing described in this chapter was carried out using IDIMS image processing software developed and marketed by ESL, Incorporated, Sunnyvale, California. The software is resident on a Hewlett Packard HP3000 minicomputer and makes use of an ESL, Incorporated, Advanced Scientific Array Processor.

The image used in the following examples was 256X256 pixels in size and had intensity values ranging from 0.0 to 255. It was an aerial image of a portion of an airport containing two complete commercial aircraft and a portion of a third, associated ground support equipment, and portions of the terminal (Figure 4.1).

Bilinear interpolation was used to magnify the original 256X256 pixel image to 512X512 pixels (Figure 4.2). The power spectrum, which is the square of the modulus of the Fourier transform, was calculated for the two images. The average power spectrum function for each image was calculated using 34 anular rings of equal width running from zero to the Nyquist frequency. The DC value was also retained. The average modulus functions were calculated from the average power spectrum functions and are shown in

Figure 4.1 Original Image

Figure 4.2 Magnified Image

Figure 4.3.

The filter for the simple filter design approach is the quotient of the original image average modulus function divided by the magnified image average modulus function. This filter function for the airport image is illustrated in Figure 4.4. The simple filter provides considerable amplification of lower frequencies that influence contrast as well as the higher frequencies that are related to sharpness. For this reason the complex filter design approach must be used to provide an output free from unwanted tonal changes. The result of the application of the simple filter is illustrated in Figure 4.5.

Figure 4.6 shows the average modulus functions for the original and magnified airport images after being processed by channel 2 of the Granrath Model. The steps undertaken to implement the channel 2 processing are as follows. First, a constant value of 1.0 was added to each pixel intensity value in the images. The natural logarithm was then taken of the intensity values. One sixth of the resulting intensity range was calculated for use later in the saturation operator. The calculated saturation level was 0.92 for both images. Next, the images were convolved with the channel 2 weighting function, $h^{(2)}-h^{(1)}$. This weighting function can be found in Appendix A. Since this function passes none of the DC level of the images, the image intensity values were then clustered around zero. Finally the intensity

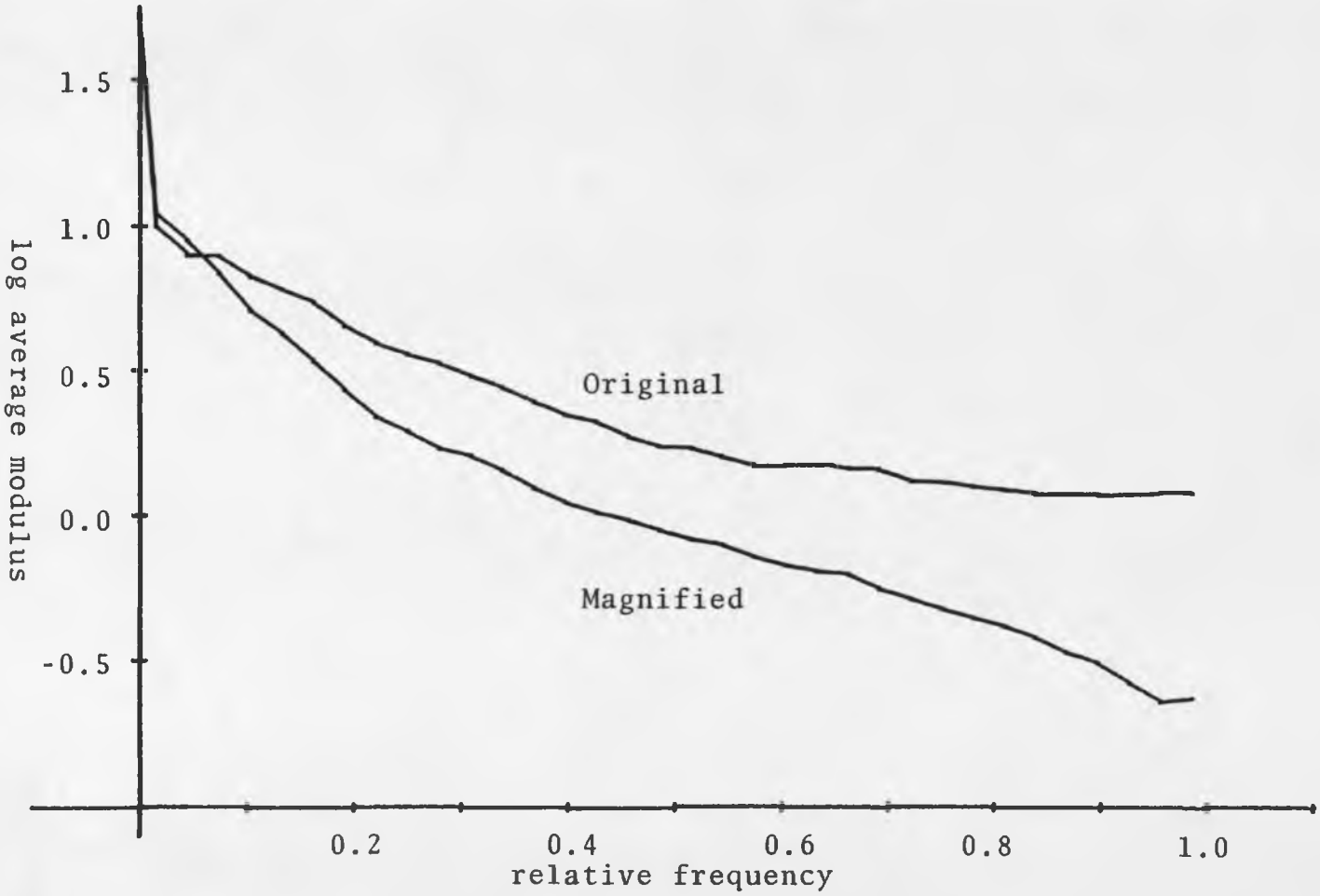

Figure 4.3 Average Modulus Functions

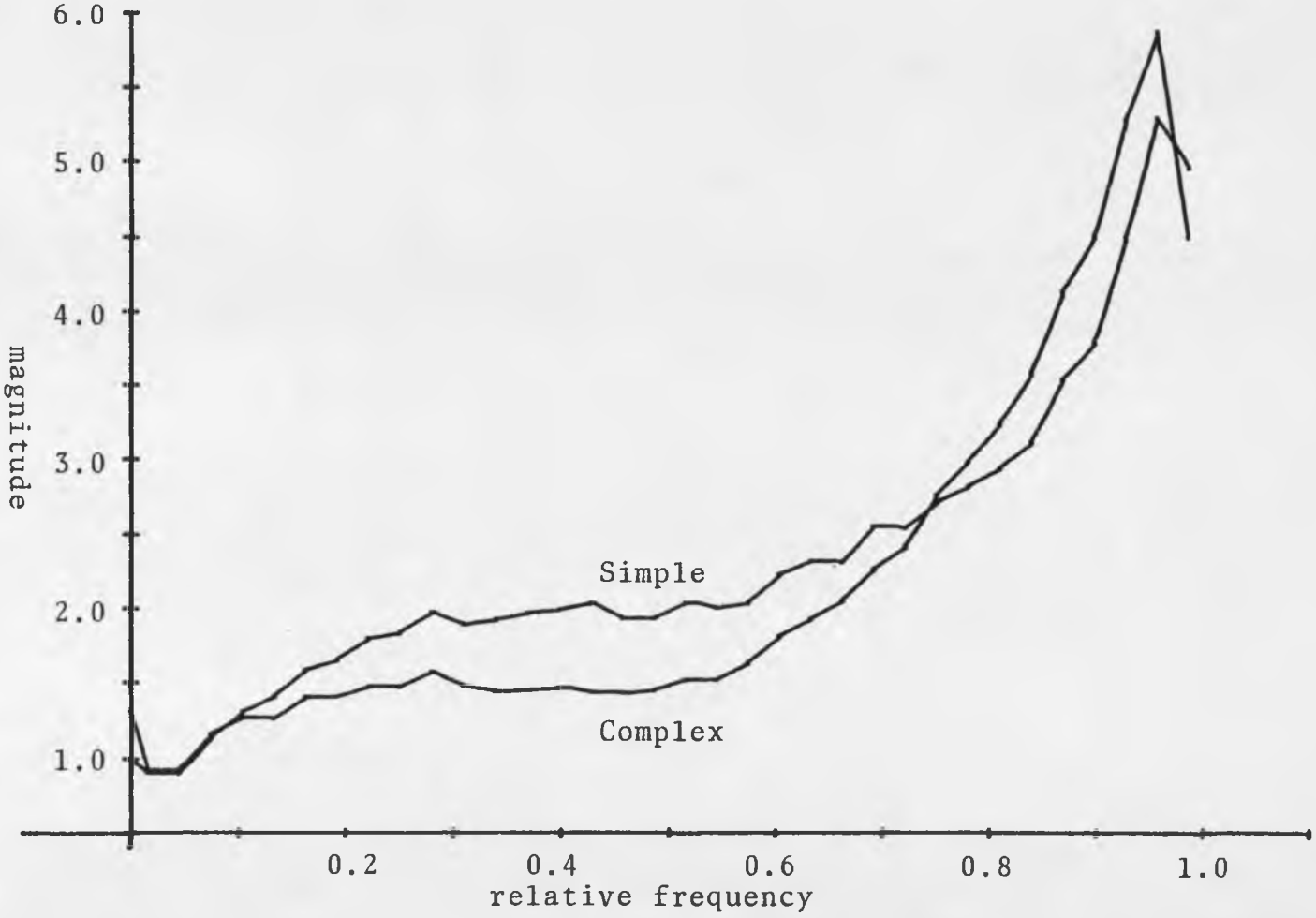

Figure 4.4 Filter Functions

Figure 4.5 Filtered Image, Simple Technique

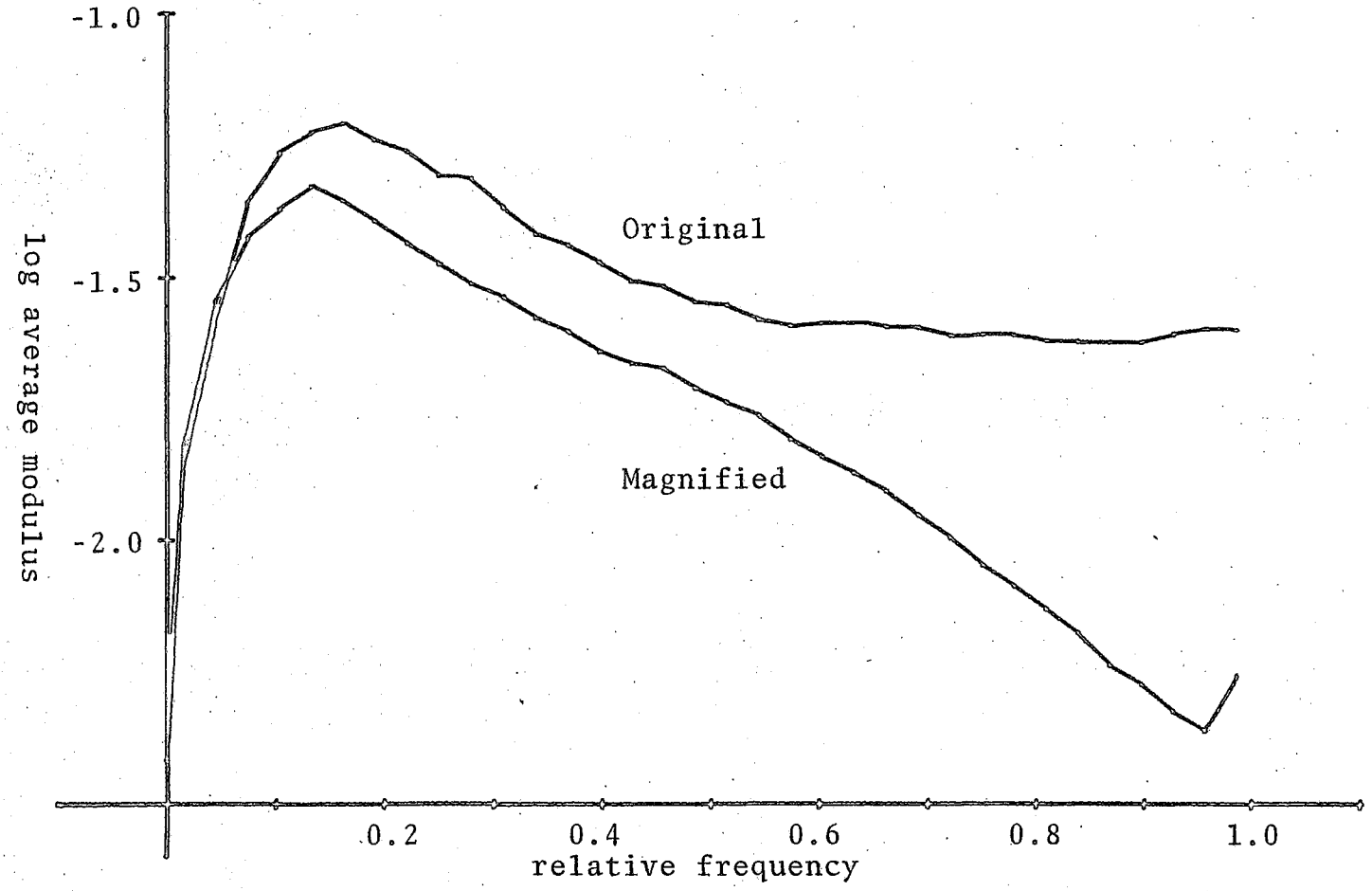

Figure 4.6 Average Modulus Functions after Granrath Model

values for both images were clipped at ±0.92 to satisfy the saturation operation. The average modulus functions were calculated for these images in the manner described earlier. The filter function developed from these preprocessed images is shown in Figure 4.4. The application of the complex filter is illustrated in Figure 4.7. One change was made to the complex filter in Figure 4.4 prior to its use. Since the DC values for the two average modulus functions in Figure 4.6 would be zero if not for roundoff errors in their calculations, the computed DC value of the complex filter (approximately 1.3) has little meaning. Intuitively you do not want to change the image mean brightness value in the filtering process so the DC value used in this application was 1.0.

The use of the complex filter design technique has provided the desired results. This filter provides less amplification of the low frequencies and greater amplification of the higher frequencies than the filter developed using the simple technique. It may be possible to tune the complex filter design technique by changing the values of the parameters in the channel 2 processing of the Granrath Model.

The image examples were written on one 70 millimeter roll of Kodak Panatomic-X film using a Dicomed Image Recorder. The film was processed in Kodak Polydol Developer. The same enlarger setting, photographic paper, and

Figure 4.7 Filtered Image, Complex Technique

paper processing was used for all the examples to reduce photographically induced differences. However, the contrast difference between the two filtered images was exaggerated, and the sharpness difference between the filtered and unfiltered magnified images was subdued by the photographic process. These changes in appearance were in relation to the images as displayed on a cathode ray tube.

CHAPTER 5

SUMMARY

The major contribution of this thesis is the use of a model of the retina to aid in the solution of a digital image processing problem. The results of this study are encouraging and may provide some incentive for the use of such vision models in the design and analysis of image processing systems.

Chapter 2 provides a description of the Granrath Model used in this study. Chapter 3 discusses the basic problem of sharpness maintenance with regard to digital image magnification and the development of restoration techniques. Chapter 4 provides an example of the filter design techniques developed in chapter 3.

This work has developed the first step in the sharpness restoration of magnified digital images, the filter design. Future studies should be oriented toward assessment of the validity of the complex filter design technique developed here through subjective analysis of the resultant output images. Once the validity is established fine tuning and streamlining of the technique can take place.

APPENDIX A

CALCULATION OF $h^{(1,2)}_{k1}$

The parameters used in the text will be applied here.

$$K = 15 \quad \text{therefore} \quad -7 \leq k \leq 7$$

$$\text{and} \quad -7 \leq \ell \leq 7$$

$$p_1 = 5.0$$

$$p_2 = 0.5$$

$$\sum_{k}\sum_{\ell} \exp\{-(k^2+\ell^2)/p_1^2\} = 73.39580554$$

$$\sum_{k}\sum_{\ell} \exp\{-(k^2+\ell^2)/p_2^2\} = 1.074604874$$

With $C_1 = C_2 = 1.0$ the equations for $h^{(1)}$ and $h^{(2)}$ are:

$$h^{(1)}_{k,\ell} = \frac{\exp\{-(k^2+\ell^2)/p_1^2\}}{73.39580554}$$

$$h^{(2)}_{k,\ell} = \frac{\exp\{-(k^2+\ell^2)/p_2^2\}}{1.074604874}$$

The results of the evaluation of these equations can be found in Tables A.1 and A.2. The combined weighting function for channel 2 of the Granrath Model is $h^{(2)}-h^{(1)}$. This function is presented in Table A.3.

Tables A.4, A.6, and A.8 contain the modulus of the Fourier transforms of $h^{(1)}$, $h^{(2)}$, and $h^{(2)}-h^{(1)}$ respectively. Tables A.5, A.7, and A.9 contain the phase values in degrees for the same Fourier transforms.

ℓ ↓ \ k	0	1	2	3	4	5	6	7
0	1.362E-02	1.309E-02	1.161E-02	9.506E-03	7.184E-03	5.012E-03	3.228E-03	1.919E-03
1	1.309E-02	1.258E-02	1.116E-02	9.133E-03	6.903E-03	4.816E-03	3.102E-03	1.844E-03
2	1.161E-02	1.116E-02	9.894E-03	8.100E-03	6.122E-03	4.271E-03	2.751E-03	1.635E-03
3	9.506E-03	9.133E-03	8.100E-03	6.632E-03	5.012E-03	3.497E-03	2.252E-03	1.339E-03
4	7.184E-03	6.903E-03	6.122E-03	5.012E-03	3.788E-03	2.643E-03	1.702E-03	1.012E-03
5	5.012E-03	4.816E-03	4.271E-03	3.497E-03	2.643E-03	1.844E-03	1.188E-03	7.060E-04
6	3.228E-03	3.102E-03	2.751E-03	2.252E-03	1.702E-03	1.188E-03	7.648E-04	4.547E-04
7	1.919E-03	1.844E-03	1.635E-03	1.339E-03	1.012E-03	7.060E-04	4.547E-04	2.703E-04

Table A.1 $h^{(1)}$

ℓ ↓ \ k	0	1	2	3	4	5	6	7
0	9.306E-01	1.704E-02	1.047E-07	2.158E-16	1.492E-28	3.462E-44	2.694E-63	7.031E-86
1	1.704E-02	3.122E-04	1.918E-09	3.953E-18	2.734E-30	6.341E-46	4.934E-65	1.288E-87
2	1.047E-07	1.918E-09	1.178E-14	2.429E-23	1.680E-35	3.896E-51	3.031E-70	7.913E-93
3	2.158E-16	3.953E-18	2.429E-23	5.007E-32	3.462E-44	8.030E-60	6.248E-79	0.000E 00
4	1.492E-28	2.734E-30	1.680E-35	3.462E-44	2.394E-56	5.552E-72	4.320E-91	0.000E 00
5	3.462E-44	6.341E-46	3.896E-51	8.030E-60	5.552E-72	1.288E-87	0.000E 00	0.000E 00
6	2.694E-63	4.934E-65	3.031E-70	6.248E-79	4.320E-91	0.000E 00	0.000E 00	0.000E 00
7	7.031E-86	1.288E-87	7.913E-93	0.000E 00	0.000E 00	0.000E 00	0.000E 00	0.000E 00

Table A.2 $h^{(2)}$

ℓ ↓ \ k	0	1	2	3	4	5	6	7
0	9.169E-01	3.954E-03	-1.161E-02	-9.506E-03	-7.184E-03	-5.012E-03	-3.228E-03	-1.919E-03
1	3.954E-03	-1.227E-02	-1.116E-02	-9.133E-03	-6.903E-03	-4.816E-03	-3.102E-03	-1.844E-03
2	-1.161E-02	-1.116E-02	-9.894E-03	-8.100E-03	-6.122E-03	-4.271E-03	-2.751E-03	-1.635E-03
3	-9.506E-03	-9.133E-03	-8.100E-03	-6.632E-03	-5.012E-03	-3.497E-03	-2.252E-03	-1.339E-03
4	-7.184E-03	-6.903E-03	-6.122E-03	-5.012E-03	-3.788E-03	-2.643E-03	-1.702E-03	-1.012E-03
5	-5.012E-03	-4.816E-03	-4.271E-03	-3.497E-03	-2.643E-03	-1.844E-03	-1.188E-03	-7.060E-04
6	-3.228E-03	-3.102E-03	-2.751E-03	-2.252E-03	-1.702E-03	-1.188E-03	-7.648E-04	-4.547E-04
7	-1.919E-03	-1.844E-03	-1.635E-03	-1.339E-03	-1.012E-03	-7.060E-04	-4.547E-04	-2.703E-04

Table A.3 $h^{(2)}-h^{(1)}$

	relative frequency							
	0.00	0.13	0.27	0.40	0.53	0.67	0.80	0.93
0.00	1.000E 00	3.724E-01	1.967E-03	7.739E-03	4.206E-03	2.363E-03	1.222E-03	3.793E-04
0.13	3.724E-01	1.386E-01	7.324E-04	2.882E-03	1.566E-03	8.799E-04	4.550E-04	1.413E-04
0.27	1.967E-03	7.324E-04	3.869E-06	1.522E-05	8.274E-06	4.648E-06	2.404E-06	7.462E-07
0.40	7.739E-03	2.882E-03	1.522E-05	5.989E-05	3.255E-05	1.829E-05	9.456E-06	2.936E-06
0.53	4.206E-03	1.566E-03	8.274E-06	3.255E-05	1.769E-05	9.940E-06	5.140E-06	1.596E-06
0.67	2.363E-03	8.799E-04	4.648E-06	1.829E-05	9.940E-06	5.584E-06	2.888E-06	8.964E-07
0.80	1.222E-03	4.550E-04	2.404E-06	9.456E-06	5.140E-06	2.888E-06	1.493E-06	4.635E-07
0.93	3.793E-04	1.413E-04	7.462E-07	2.936E-06	1.596E-06	8.964E-07	4.635E-07	1.439E-07
1.07	3.793E-04	1.413E-04	7.462E-07	2.936E-06	1.596E-06	8.964E-07	4.635E-07	1.439E-07
1.20	1.222E-03	4.550E-04	2.404E-06	9.456E-06	5.140E-06	2.888E-06	1.493E-06	4.635E-07
1.33	2.363E-03	8.799E-04	4.648E-06	1.829E-05	9.940E-06	5.584E-06	2.888E-06	8.964E-07
1.47	4.206E-03	1.566E-03	8.274E-06	3.255E-05	1.769E-05	9.940E-06	5.140E-06	1.596E-06
1.60	7.739E-03	2.882E-03	1.522E-05	5.989E-05	3.255E-05	1.829E-05	9.456E-06	2.936E-06
1.73	1.967E-03	7.324E-04	3.869E-06	1.522E-05	8.274E-06	4.648E-06	2.404E-06	7.462E-07
1.87	3.724E-01	1.386E-01	7.324E-04	2.882E-03	1.566E-03	8.799E-04	4.550E-04	1.413E-04

Table A.4 $h^{(1)}$ Fourier Transform Modulus

	relative frequency							
	0.00	0.13	0.27	0.40	0.53	0.67	0.80	0.93
0.00	0.000E 00	1.200E 01	2.400E 01	3.600E 01	4.800E 01	6.000E 01	7.200E 01	8.400E 01
0.13	1.200E 01	2.400E 01	3.600E 01	4.800E 01	6.000E 01	7.200E 01	8.400E 01	-8.400E 01
0.27	2.400E 01	3.600E 01	4.800E 01	6.000E 01	7.200E 01	8.400E 01	-8.400E 01	-7.200E 01
0.40	3.600E 01	4.800E 01	6.000E 01	7.200E 01	8.400E 01	-8.400E 01	-7.200E 01	-6.000E 01
0.53	4.800E 01	6.000E 01	7.200E 01	8.400E 01	-8.400E 01	-7.200E 01	-6.000E 01	-4.800E 01
0.67	6.000E 01	7.200E 01	8.400E 01	-8.400E 01	-7.200E 01	-6.000E 01	-4.800E 01	-3.600E 01
0.80	7.200E 01	8.400E 01	-8.400E 01	-7.200E 01	-6.000E 01	-4.800E 01	-3.600E 01	-2.400E 01
0.93	8.400E 01	-8.400E 01	-7.200E 01	-6.000E 01	-4.800E 01	-3.600E 01	-2.400E 01	-1.200E 01
1.07	-8.400E 01	-7.200E 01	-6.000E 01	-4.800E 01	-3.600E 01	-2.400E 01	-1.200E 01	-3.307E-04
1.20	-7.200E 01	-6.000E 01	-4.800E 01	-3.600E 01	-2.400E 01	-1.200E 01	-1.436E-04	1.200E 01
1.33	-6.000E 01	-4.800E 01	-3.600E 01	-2.400E 01	-1.200E 01	-6.016E-05	1.200E 01	2.400E 01
1.47	-4.800E 01	-3.600E 01	-2.400E 01	-1.200E 01	-2.675E-06	1.200E 01	2.400E 01	3.600E 01
1.60	-3.600E 01	-2.400E 01	-1.200E 01	-4.709E-06	1.200E 01	2.400E 01	3.600E 01	4.800E 01
1.73	-2.400E 01	-1.200E 01	-1.327E-05	1.200E 01	2.400E 01	3.600E 01	4.800E 01	6.000E 01
1.87	-1.200E 01	4.670E-10	1.200E 01	2.400E 01	3.600E 01	4.800E 01	6.000E 01	7.200E 01

Table A.5 $h^{(1)}$ Fourier Transform Phase

	relative frequency							
	0.00	0.13	0.27	0.40	0.53	0.67	0.80	0.93
0.00	1.000E 00	9.969E-01	9.883E-01	9.756E-01	9.610E-01	9.470E-01	9.361E-01	9.301E-01
0.13	9.969E-01	9.939E-01	9.853E-01	9.726E-01	9.580E-01	9.441E-01	9.332E-01	9.273E-01
0.27	9.883E-01	9.853E-01	9.768E-01	9.642E-01	9.497E-01	9.359E-01	9.251E-01	9.192E-01
0.40	9.756E-01	9.726E-01	9.642E-01	9.518E-01	9.375E-01	9.239E-01	9.132E-01	9.074E-01
0.53	9.610E-01	9.580E-01	9.497E-01	9.375E-01	9.235E-01	9.100E-01	8.995E-01	8.938E-01
0.67	9.470E-01	9.441E-01	9.359E-01	9.239E-01	9.100E-01	8.968E-01	8.865E-01	8.808E-01
0.80	9.361E-01	9.332E-01	9.251E-01	9.132E-01	8.995E-01	8.865E-01	8.762E-01	8.706E-01
0.93	9.301E-01	9.273E-01	9.192E-01	9.074E-01	8.938E-01	8.808E-01	8.706E-01	8.651E-01
1.07	9.301E-01	9.273E-01	9.192E-01	9.074E-01	8.938E-01	8.808E-01	8.706E-01	8.651E-01
1.20	9.361E-01	9.332E-01	9.251E-01	9.132E-01	8.995E-01	8.865E-01	8.762E-01	8.706E-01
1.33	9.470E-01	9.441E-01	9.359E-01	9.239E-01	9.100E-01	8.968E-01	8.865E-01	8.808E-01
1.47	9.610E-01	9.580E-01	9.497E-01	9.375E-01	9.235E-01	9.100E-01	8.995E-01	8.938E-01
1.60	9.756E-01	9.726E-01	9.642E-01	9.518E-01	9.375E-01	9.239E-01	9.132E-01	9.074E-01
1.73	9.883E-01	9.853E-01	9.768E-01	9.642E-01	9.497E-01	9.359E-01	9.251E-01	9.192E-01
1.87	9.969E-01	9.939E-01	9.853E-01	9.726E-01	9.580E-01	9.441E-01	9.332E-01	9.273E-01

Table A.6 $h^{(2)}$ Fourier Transform Modulus

	relative frequency							
	0.00	0.13	0.27	0.40	0.53	0.67	0.80	0.93
0.00	0.000E 00	1.200E 01	2.400E 01	3.600E 01	4.800E 01	6.000E 01	7.200E 01	8.400E 01
0.13	1.200E 01	2.400E 01	3.600E 01	4.800E 01	6.000E 01	7.200E 01	8.400E 01	-8.400E 01
0.27	2.400E 01	3.600E 01	4.800E 01	6.000E 01	7.200E 01	8.400E 01	-8.400E 01	-7.200E 01
0.40	3.600E 01	4.800E 01	6.000E 01	7.200E 01	8.400E 01	-8.400E 01	-7.200E 01	-6.000E 01
0.53	4.800E 01	6.000E 01	7.200E 01	8.400E 01	-8.400E 01	-7.200E 01	-6.000E 01	-4.800E 01
0.67	6.000E 01	7.200E 01	8.400E 01	-8.400E 01	-7.200E 01	-6.000E 01	-4.800E 01	-3.600E 01
0.80	7.200E 01	8.400E 01	-8.400E 01	-7.200E 01	-6.000E 01	-4.800E 01	-3.600E 01	-2.400E 01
0.93	8.400E 01	-8.400E 01	-7.200E 01	-6.000E 01	-4.800E 01	-3.600E 01	-2.400E 01	-1.200E 01
1.07	-8.400E 01	-7.200E 01	-6.000E 01	-4.800E 01	-3.600E 01	-2.400E 01	-1.200E 01	-1.700E-14
1.20	-7.200E 01	-6.000E 01	-4.800E 01	-3.600E 01	-2.400E 01	-1.200E 01	-8.062E-12	1.200E 01
1.33	-6.000E 01	-4.800E 01	-3.600E 01	-2.400E 01	-1.200E 01	-1.731E-12	1.200E 01	2.400E 01
1.47	-4.800E 01	-3.600E 01	-2.400E 01	-1.200E 01	1.097E-12	1.200E 01	2.400E 01	3.600E 01
1.60	-3.600E 01	-2.400E 01	-1.200E 01	-2.970E-12	1.200E 01	2.400E 01	3.600E 01	4.800E 01
1.73	-2.400E 01	-1.200E 01	-8.639E-14	1.200E 01	2.400E 01	3.600E 01	4.800E 01	6.000E 01
1.87	-1.200E 01	2.308E-13	1.200E 01	2.400E 01	3.600E 01	4.800E 01	6.000E 01	7.200E 01

Table A.7 $h^{(2)}$ Fourier Transform Phase

	relative frequency							
	0.00	0.13	0.27	0.40	0.53	0.67	0.80	0.93
0.00	3.943E-12	6.246E-01	9.903E-01	9.678E-01	9.652E-01	9.446E-01	9.373E-01	9.297E-01
0.13	6.246E-01	8.553E-01	9.860E-01	9.697E-01	9.596E-01	9.432E-01	9.337E-01	9.271E-01
0.27	9.903E-01	9.860E-01	9.767E-01	9.642E-01	9.497E-01	9.359E-01	9.251E-01	9.192E-01
0.40	9.678E-01	9.697E-01	9.642E-01	9.517E-01	9.375E-01	9.239E-01	9.132E-01	9.074E-01
0.53	9.652E-01	9.596E-01	9.497E-01	9.375E-01	9.234E-01	9.100E-01	8.995E-01	8.938E-01
0.67	9.446E-01	9.432E-01	9.359E-01	9.239E-01	9.100E-01	8.968E-01	8.865E-01	8.808E-01
0.80	9.373E-01	9.337E-01	9.251E-01	9.132E-01	8.995E-01	8.865E-01	8.762E-01	8.706E-01
0.93	9.297E-01	9.271E-01	9.192E-01	9.074E-01	8.938E-01	8.808E-01	8.706E-01	8.651E-01
1.07	9.297E-01	9.271E-01	9.192E-01	9.074E-01	8.938E-01	8.808E-01	8.706E-01	8.651E-01
1.20	9.373E-01	9.337E-01	9.251E-01	9.132E-01	8.995E-01	8.865E-01	8.762E-01	8.706E-01
1.33	9.446E-01	9.432E-01	9.359E-01	9.239E-01	9.100E-01	8.968E-01	8.865E-01	8.808E-01
1.47	9.652E-01	9.596E-01	9.497E-01	9.375E-01	9.234E-01	9.100E-01	8.995E-01	8.938E-01
1.60	9.678E-01	9.697E-01	9.642E-01	9.517E-01	9.375E-01	9.239E-01	9.132E-01	9.074E-01
1.73	9.903E-01	9.860E-01	9.767E-01	9.642E-01	9.497E-01	9.359E-01	9.251E-01	9.192E-01
1.87	6.246E-01	8.553E-01	9.860E-01	9.697E-01	9.596E-01	9.432E-01	9.337E-01	9.271E-01

Table A.8 $h^{(2)}$-$h^{(1)}$ Fourier Transform Modulus

	relative frequency							
	0.00	0.13	0.27	0.40	0.53	0.67	0.80	0.93
0.00	0.000E 00	1.200E 01	2.400E 01	3.600E 01	4.800E 01	6.000E 01	7.200E 01	8.400E 01
0.13	1.200E 01	2.400E 01	3.600E 01	4.800E 01	6.000E 01	7.200E 01	8.400E 01	-8.400E 01
0.27	2.400E 01	3.600E 01	4.800E 01	6.000E 01	7.200E 01	8.400E 01	-8.400E 01	-7.200E 01
0.40	3.600E 01	4.800E 01	6.000E 01	7.200E 01	8.400E 01	-8.400E 01	-7.200E 01	-6.000E 01
0.53	4.800E 01	6.000E 01	7.200E 01	8.400E 01	-8.400E 01	-7.200E 01	-6.000E 01	-4.800E 01
0.67	6.000E 01	7.200E 01	8.400E 01	-8.400E 01	-7.200E 01	-6.000E 01	-4.800E 01	-3.600E 01
0.80	7.200E 01	8.400E 01	-8.400E 01	-7.200E 01	-6.000E 01	-4.800E 01	-3.600E 01	-2.400E 01
0.93	8.400E 01	-8.400E 01	-7.200E 01	-6.000E 01	-4.800E 01	-3.600E 01	-2.400E 01	-1.200E 01
1.07	-8.400E 01	-7.200E 01	-6.000E 01	-4.800E 01	-3.600E 01	-2.400E 01	-1.200E 01	5.502E-11
1.20	-7.200E 01	-6.000E 01	-4.800E 01	-3.600E 01	-2.400E 01	-1.200E 01	2.402E-10	1.200E 01
1.33	-6.000E 01	-4.800E 01	-3.600E 01	-2.400E 01	-1.200E 01	3.822E-10	1.200E 01	2.400E 01
1.47	-4.800E 01	-3.600E 01	-2.400E 01	-1.200E 01	5.125E-11	1.200E 01	2.400E 01	3.600E 01
1.60	-3.600E 01	-2.400E 01	-1.200E 01	3.084E-10	1.200E 01	2.400E 01	3.600E 01	4.800E 01
1.73	-2.400E 01	-1.200E 01	5.256E-11	1.200E 01	2.400E 01	3.600E 01	4.800E 01	6.000E 01
1.87	-1.200E 01	1.139E-11	1.200E 01	2.400E 01	3.600E 01	4.800E 01	6.000E 01	7.200E 01

Table A.9 $h^{(2)}$-$h^{(1)}$ Fourier Transform Phase

REFERENCES

Andrews, H. C. and B. R. Hunt. Digital Image Restoration. Prentice-Hall, Inc., Englewood Cliffs, New Jersey, 1977.

Granrath, D. J. "Models of human vision in digital image bandwidth compression." Dissertation, University of Arizona, Tucson, Arizona, 1979.

Granrath, D. J. and B. R. Hunt. "A two-channel model of image processing in the human retina." SPIE Proceedings, Advances in Display Technology, Vol. 199, (1979), pp. 126-133.

Hall, C. F. and E. L. Hall. "A nonlinear model for the spacial characteristics of the human visual system." IEEE Transactions on Systems, Man, and Cybernetics, Vol. SMC-7, No. 3, (March 1977), pp. 161-170.

Hunt, B. R. and G. F. Sera. "Power-law stimulus-response models for measures of image quality in non-performance environments." IEEE Transactions on Systems, Man, and Cybernetics, Vol. SMC-8, No. 11, (November 1978), pp. 781-791.

Legge, G. E. "Sustained and transient mechanisms in human vision: temporal and spacial properties." Vision Research, Vol. 18, (1978), pp. 69-81.

Mannos, J. L. and D. J. Sakrison. "The effects of a visual fidelity criterion on the encoding of images." IEEE Transactions on Information Theory, Vol. IT-20, No. 4, (July 1974), pp. 525-536.

Pratt, W. K. Digital Image Processing. Wiley and Sons, New York, 1978.